Unconventional vortex dynamics in superconducting states with broken time-reversal symmetry

Elisabeth Dumont and Ana Celia Mota
Laboratorium für Festkörperphysik, ETH Zürich, 8093 Zürich, Switzerland
(Received 1 October 2001; revised manuscript received 21 December 2001; published 2 April 2002)

We report vortex dynamics in the unconventional superconductors Sr_2RuO_4, thoriated UBe_{13} and compare it with previous data on UPt_3 [A. Amann, A. C. Mota, M. B. Maple, and H.v. Löhneysen, Phys. Rev. B **57**, 3640 (1998)]. In all three systems, a pinning mechanism, which is very distinct from the standard pinning by defects, can be associated with the appearance of broken time-reversal symmetry in the superconducting state. The pinning mechanism is so strong that no vortex creep is observed in a time scale of several hours. Our observations could be explained by the presence of domain walls, separating different degenerate superconducting states, as proposed by Sigrist and Agterberg [Prog. Theor. Phys. **102**, 965 (1999)]. A conventional vortex approaching such a domain wall can decay into vortices with fractional flux quanta. Domain walls occupied with strongly pinned fractional vortices, represent efficient barriers for vortex motion and thus prevent relaxation towards equilibrium. In the case of UPt_3 and $U_{0.9725}Th_{0.0275}Be_{13}$, two consecutive phase transitions are known to occur at $H=0$, of which the low temperature one leads to a superconducting phase with broken time-reversal symmetry. In both systems, one observes a sharp drop of initial creep rates by more than three orders of magnitude to undetectabely low levels at their second superconducting transition. In Sr_2RuO_4 time-reversal symmetry is reported to occur right below T_c. However, we do not observe unconventional pinning immediately below the superconducting transition, but zero creep sets in only much below T_c. While in $U_{0.9725}Th_{0.0275}Be_{13}$ and UPt_3, the drop in creep rates at the lower superconducting transition temperature is very sudden and strong, in Sr_2RuO_4 it looks more like a *crossover*.

DOI: 10.1103/PhysRevB.65.144519 PACS number(s): 74.60.Ge

I. INTRODUCTION

In superconductors the physical manifestation of time-reversal symmetry ($\mathcal{T}$) breaking are starting to be considered from a theoretical point of view as well as from experiments. The breakdown of $\mathcal{T}$ is a well-known property of ferromagnets. Since it was a long-believed fact that magnetism and superconductivity would exclude each other, the more intriguing was the evidence for time-reversal symmetry breaking in unconventional superconductors. Up to some years ago, the only known condensate with broken time-reversal symmetry was the *A* phase of superfluid ^{3}He.[1,2] Nowadays, there are three examples of unconventional superconducting phases that very likely violate $\mathcal{T}$. They are the low-temperature superconducting phases of the two heavy fermion metals UPt_3 (Ref. 3) and $U_{1-x}Th_xBe_{13}$ with $0.019<x<0.045$,[4,5] and the recently discovered superconductor Sr_2RuO_4.[6] We present here a study of time-reversal-symmetry-breaking superconducting states using vortices as a probe.

A type-II superconductor in a magnetic field higher than its lower critical field, is threaded by quantized magnetic-flux lines. Each line carries a single flux quantum $\Phi_o=hc/2e$. In conventional superconductors this is the only form for a vortex. However, in analogy to rotating superfluid ^{3}He, where seven different types of vortices have been identified in the *A* and *B* phases,[7] new and interesting vortex physics is to be expected in unconventional superconductors.[8] Since in the latter, the superconducting order parameter has more than one component, this yields many more degrees of freedom to form topologically stable defects.

In superconductors with a multicomponent order parameter, domain walls separating different degenerate superconducting states form. As discussed by Sigrist and Agterberg, a conventional vortex approaching such a domain wall can decay into fractional vortices. Due to vortex-vortex repulsion, domain walls occupied with pinned fractional vortices, represent efficient barriers for vortex motion and thus prevent flux flow.[9] The heavy fermion systems UPt_3 and $U_{1-x}Th_xBe_{13}$ (with $0.019<x<0.045$) are up to now the only known examples of superconductors that show more than one superconducting phase. The phase diagram of UPt_3 is shown in Fig. 1. It contains three different superconducting phases, labeled *A*, *B*, and *C*, which meet at a tetracritical point. Muon-spin-resonance (μSR) measurements have given evidence that the low temperature, low-field *B* phase of UPt_3 violates time-reversal symmetry.[3]

The phase diagram of $U_{1-x}Th_xBe_{13}$ is given in Fig. 2. The

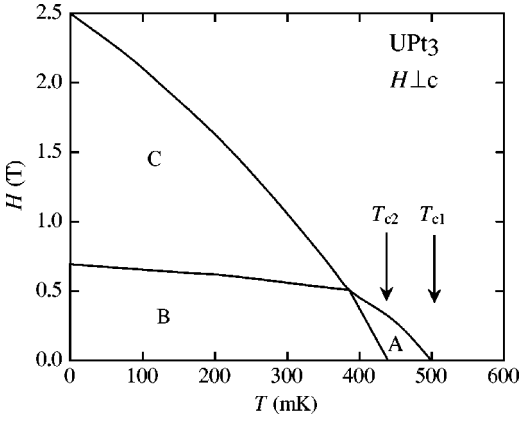

FIG. 1. Phase diagram of UPt_3 for fields in the basal plane. Three different superconducting phases, labeled *A*, *B*, and *C*, have been identified. They meet at a tetracritical point.

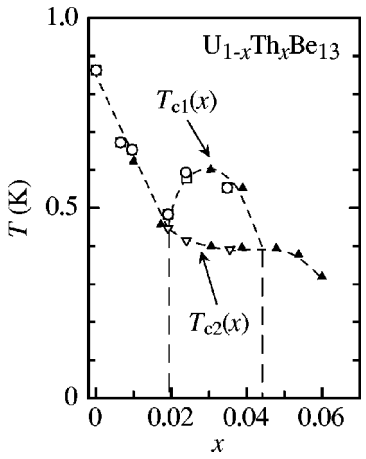

FIG. 2. Phase diagram of $U_{1-x}Th_xBe_{13}$, after Ref. 5.

critical temperature exhibits an unsual nonmonotonic behavior as a function of thorium concentration. It has a sharp minimum at $x_1 \approx 0.019$ and an additional irregular point has been proposed at $x_2 \approx 0.045$. In this critical-concentration regime, $x_1 < x < x_2$, a second superconducting phase transition occurs at T_{c2}. Heffner *et al.* observed an increase of zero-field μSR relaxation rate that sets in at T_{c2} and is restricted only to concentrations in the critical regime.[4] This result was attributed to the breakdown of time-reversal symmetry in the low-temperature superconducting phase.[10]

Similar to the observations of Amann *et al.* in UPt_3,[11] we observe in thoriated UBe_{13} in the critical-concentration regime, an unusually sharp drop of initial creep rates by more than three orders of magnitude to zero, within our sensitivity ($|\partial \ln M/\partial \ln t| \approx 2\times 10^{-6}$). This abrupt reduction of creep rates coincides with the second superconducting transition at T_{c2}.[12–14]

A multicomponent order parameter is most certainly also realized in Sr_2RuO_4, a material structurally similar to the high-T_c superconductor $(La_{1-x}Sr_x)_2CuO_4$ but with a much lower T_c of 1.5 K. Indeed, shortly after its discovery in 1994,[15] Rice and Sigrist[16,17] proposed that *p*-wave superconductivity might be realized in Sr_2RuO_4. Zero-field muon spin relaxation revealed the breakdown of time-reversal symmetry below T_c.[6]

In Sr_2RuO_4 we do not observe ''zero creep'' immediately below the superconducting transition. However, a regime with unconventional strong pinning similar to the one in the low-temperature phases of $U_{0.9725}Th_{0.0275}Be_{13}$ and UPt_3 sets in much below T_c.[18] While in these heavy electron systems the drop in creep rates at the lower superconducting transition temperature is very sudden and strong, in Sr_2RuO_4 it looks more like a crossover. Up to now, there is no experimental evidence for a second phase transition in this last superconductor.

II. EXPERIMENTAL DETAILS

A. Measuring setup

Both ac-susceptibility and dc-magnetization measurements have been performed, in a temperature range between 7 mK and 2 K, using a custom-made rf-SQUID (superconducting quantum interference device) magnetometer, built inside a $^3He/^4He$ dilution refrigerator. The cryostat is based on a commercial model, where the copper mixing chamber has been extended by a custom-made experimental cell, such that the sample is in direct contact with the $^3He/^4He$ mixture. In our system the sample remains stationary inside the gradiometer coils during the whole measurement. No superconducting shielding is used in the coil system and neither of the coils are used in persistent mode. The residual field at the sample space has been measured to be less than 2 mOe. The dc field can be varied up to about 2500 Oe. For the ac-susceptibility measurements, an ac-impedance bridge with a SQUID as a null detector is used. The amplitude of the ac field is variable in fixed steps between 0.07 and 33 mOe, and its frequency can be set at 16, 32, 80, or 160 Hz. The dc- and ac-fields are applied parallel to each other. The experimental arrangement has been described in detail in Ref. 19.

B. Measuring procedure

We have studied vortex dynamics by means of relaxation measurements of the remnant magnetization from a metastable configuration originating from the application of a magnetic field. Isothermal relaxation measurements have been performed at different temperatures and cycling fields. First the sample has been zero-field cooled to the desired temperature. Then, the field has been raised to a maximum value H_{max} within $\approx$1 min. After a waiting time of a few seconds at this maximum cycling field, the field has been reduced to zero within seconds. The remnant magnetization is recorded as a function of time, the starting time $t=0$ being defined as the moment when the external field reaches zero. Relaxation measurements have typically been performed in the time window between 1 s and 10^4 s or 10^5 s. After each decay measurement, the sample is heated above its superconducting transition temperature and the expelled flux is recorded as a function of temperature. The remnant magnetization is obtained as the sum of the flux leaving the sample during decay and subsequent expulsion.

C. Samples

1. $U_{0.9725}Th_{0.0275}Be_{13}$ single crystal

The single crystal of $U_{0.9725}Th_{0.0275}Be_{13}$ has been prepared at Los Alamos National Laboratory.[20] It has the form of a parallelepiped with dimensions 2.3 mm$\times$0.9 mm$\times$1.0 mm and mass 8 mg. The magnetic field was applied to the sample along the (100) plane, which corresponds to the sample's largest dimension. The critical temperature of the sample, obtained by ac-susceptibility measurements, takes place at $T_{c1}=523$ mK and has a width $\Delta T_{c1}=67$ mK. T_{c1} has been taken as the midpoint of the transition and the value for ΔT_{c1} has been obtained by the 10–90 % criterion. Specific-heat measurements performed on a sample of the same batch[21] revealed a second jump at $T_{c2}=350$ mK with a width $\Delta T_{c2}=40$ mK.

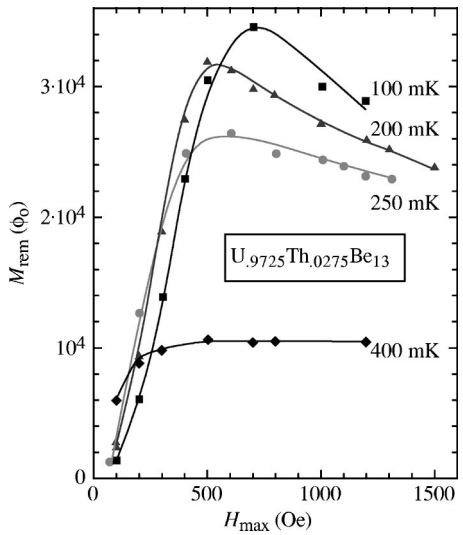

FIG. 3. Dependence of the remnant magnetization of the $U_{0.9725}Th_{0.0275}Be_{13}$ single crystal on the maximum cycling field, for different temperatures. The lines serve as guides to the eyes.

2. Sr_2RuO_4 single crystals

For the work presented here, two Sr_2RuO_4 single crystals with different transition temperatures have been measured. Both crystals were prepared by the floating-zone technique[15] by Maeno *et al.* at Kyoto University.

Sample *A* has an almost ellipsoidal shape with dimensions 2.63 mm×1.52 mm×0.98 mm and mass 11.5 mg. It was oriented by Laue x-ray diffraction. In the first series of measurements, the field has been applied perpendicular to the sample's largest dimension, i.e., at an angle of 15° from the ab plane. Second, it has been applied parallel to the c axis. The superconducting transition of the sample takes place at $T_c = 1.03\ K$ and has a width $\Delta T_c = 300$ mK.

Sample *B* is a rather big parallelepiped with rounded corners, of dimensions 4.8 mm×2.2 mm×2.6 mm and mass 129 mg. It has been oriented with the help of electron-channeling diagrams. Susceptibility measurements gave $T_c = 1.4$ K with a width $\Delta T_c = 230$ mK. The field has been applied along the ab plane.

III. EXPERIMENTAL RESULTS

A. Flux dynamics in thoriated UBe_{13}

1. Remnant magnetization as a function of temperature and field

The field dependence of the remnant magnetization is very distinct in the low-temperature and high-temperature superconducting phases of $U_{0.9725}Th_{0.0275}Be_{13}$, as can be seen in Fig. 3. In the latter the remnant magnetization is plotted for different temperatures both below, and above T_{c2}.

$T > T_{c2}$. At $T = 400$ mK, the remnant magnetization follows the classical behavior as described by the Bean model.[25] For low fields, M_{rem} increases as a function of H_{max} until H_{max} reaches the value $2H^* \approx 400$ Oe. For fields $H > 2H^*$, the remnant magnetization M_{rem} becomes independent of H_{max}, i.e., the sample is in the fully critical state.

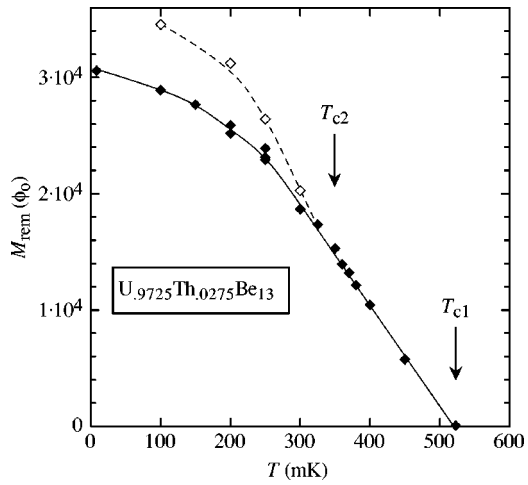

FIG. 4. Values of the remnant magnetization M_{rem} of the $U_{0.9725}Th_{0.0275}Be_{13}$ single crystal as a function of temperature. For temperatures $T < T_{c2}$, values of M_{rem} at $H = 1200$ Oe (closed diamonds), and the maximum value of M_{rem} as a function of H_{max} (open diamonds) are plotted. The line serves as guide to the eyes.

$T < T_{c2}$. In the low-temperature phase on the other hand, the field dependence of the remnant magnetization is very distinct from that expected by the Bean model. M_{rem} does not saturate as a function of field. For increasing fields H_{max}, the remnant magnetization M_{rem} first increases, goes through a maximum and then decreases again with further increasing field. This indicates a field-induced ''memory effect'' in vortex pinning. It results in a different critical state at $H = 0$ depending on the maximum field to which the sample has been cycled.

In Fig. 4, M_{rem} is given as a function of temperature, for the cycling field $H = 1200$ Oe (closed diamonds), and the maximum value of $M_{rem}(H)$ (open diamonds). For $T < T_{c2}$, the simple identification of M_{rem} with the critical current breaks down.

2. Relaxation measurements as a function of temperature

Studies of vortices and their dynamics in classical hard type-II superconductors have a long history on account of their technological importance. A type-II superconductor carrying a current is in a thermodynamically metastable state, which decays towards equilibrium as a result of thermally activated motion of vortices. This phenomenon has been observed by Kim *et al.*[22] and described by Anderson.[23]

Figure 5 shows typical relaxation measurements of the remnant magnetization of $U_{0.9725}Th_{0.0275}Be_{13}$ as a function of temperature. For temperatures below T_{c2}, we plotted the decays taken after the sample has been cycled to a field larger than the one, where M_{rem} takes its maximum value (see Fig. 3). The field dependence of the relaxation measurements will be discussed in Sec. III A 3.

$T > T_{c2}$. Rather strong vortex creep is observed (about 30% at $T = 400$ mK after 10^5 s), which follows an almost logarithmic time dependence. Logarithmic decays of vortices have been observed in conventional superconductors, in or-

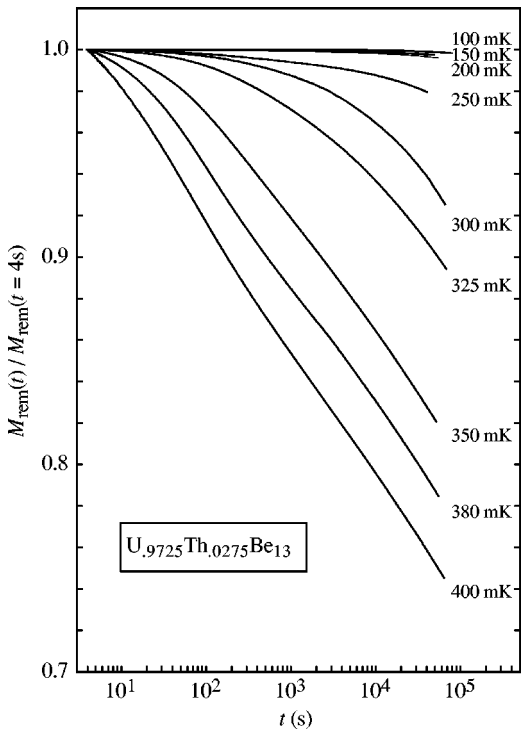

FIG. 5. Relaxation of the remnant magnetization of the $U_{0.9725}Th_{0.0275}Be_{13}$ single crystal at different temperatures.

ganics and in high-T_c cuprates, as a result of thermally activated vortex creep.[23]

$T<T_{c2}$. The decays start deviating from this logarithmic time behavior. First, the initial decay is strongly reduced, so that for short times, almost no vortex creep is observed. Second, after some waiting time, the relaxation recovers and the vortex creep accelerates. As the temperature is more and more reduced below T_{c2}, these accelerations occur at longer and longer times. Far inside the low-temperature phase, at $T \ll T_{c2}$, the vortices remain so strongly pinned that no creep is observed in our time window (10^4 s–10^5 s).

Immediately below the second transition, the decays show a strong deviation from the logarithmic time dependence. However, in order to compare different samples, we have choosen to characterize the decays of $U_{0.9725}Th_{0.0275}Be_{13}$ by two parameters: (i) the initial logarithmic slope of M vs t, which gives us the *initial* creep rates $|\partial \ln M/\partial \ln t|$, and (ii) the deviation from the logarithmic time dependence $\Delta M/M_{rem}$ at 10^4 seconds. This choice might seem arbitrary, but it affects mainly the relaxation data around the transition $T_{c2}=350$ mK. It does not influence the data at much higher or much lower temperatures, as can be seen from Fig. 6. In this graph, we have plotted the normalized deviation $\Delta M/M_{rem}(t=10^4$ s) from the logarithmic time law as a function of temperature. In the high-temperature phase, a small temperature-independent deviation from a purely logarithmic decay occurs at longer times ($t>10^3$ s). The deviation is very pronounced around T_{c2}, which is due to nonlogarithmic decays in this temperature region. At very low temperatures $T \leqslant 200$ mK, on the other hand, $\Delta M/M_{rem}(t=10^4$ s) is practically zero. In this temperature region, vortices remain so strongly pinned, that they do not manage to escape from the sample.

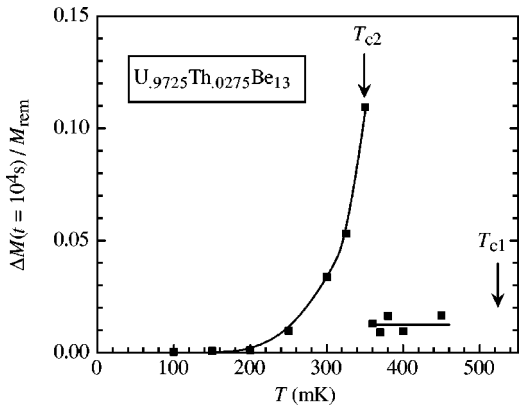

FIG. 6. Deviation of the decays of the $U_{0.9725}Th_{0.0275}Be_{13}$ single crystal from the logarithmic time law at $t=10^4$ s as a function of temperature. The deviation is very pronounced just below the second transition temperature $T_{c2}=350$ mK, but negligible above and much below the transition.

This lack of creep indicates an unusal strong pinning mechanism that sets in below the second transition temperature and inhibits flux motion. From Fig. 6, it becomes also clear, that the pinning mechanism increases gradually with decreasing temperature below T_{c2}. Far inside the low-temperature phase it is so strong, that vortex creep is reduced to practically zero within our time window. We refer to this phenomenon as ''zero creep.''

The initial creep rates are plotted in Fig. 7 as a function of temperature together with the measured lower critical field data.[13] At $T=T_{c2}$, we observe a sharp transition in the initial creep rates. Note that the transition in creep rates coincides with the break in the lower critical field, observed also by other authors.[24] At T_{c2}, the rates drop by three orders of magnitude to zero within our sensitivity ($|\partial \ln M/\partial \ln t| \approx 2 \times 10^{-6}$). Our sensitivity is limited mainly by the reproducibility of the background creep of the NbTi coils that are at

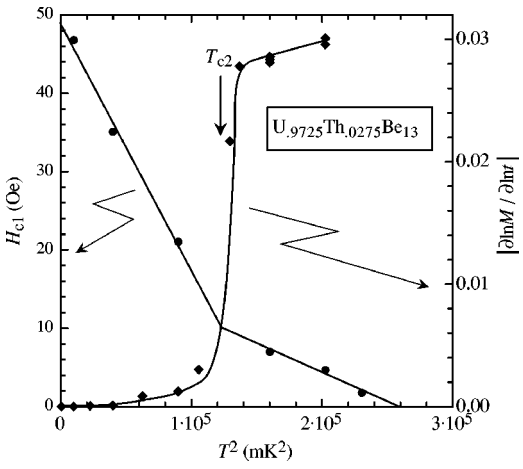

FIG. 7. Lower critical field H_{c1} (closed circles, left scale) and normalized initial creep rates $|\partial \ln M/\partial \ln t|$ (closed diamonds, right scale) of the $U_{0.9725}Th_{0.0275}Be_{13}$ single crystal. The line serves as guide to the eyes.

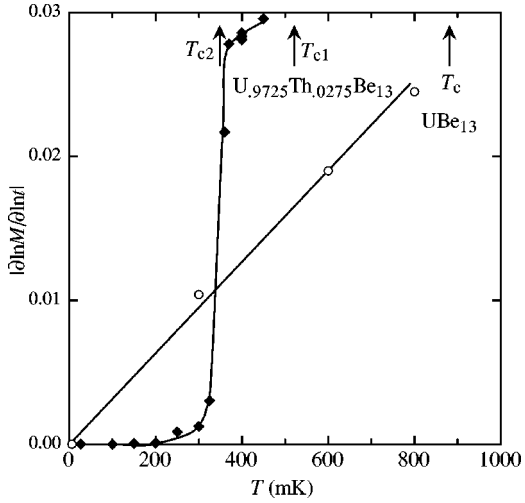

FIG. 8. Normalized creep rates of the thoriated (closed diamonds) and the pure UBe_{13} (open circles) single crystals. The transition temperatures of $U_{0.9725}Th_{0.0275}Be_{13}$, T_{c1} and T_{c2}, are marked, as well as the critical temperature of the UBe_{13} sample.

about the same temperature as the sample.

It is interesting to compare these results to those obtained by Amann *et al.*[11] on pure UBe_{13}. According to the phase diagram in Fig. 2, the pure compound exhibits a single superconducting phase. Moreover, there is no experimental evidence that it violates time reversal symmetry. In Fig. 8, we give vortex creep rates of pure UBe_{13} and vortex creep rates of $U_{0.9725}Th_{0.0275}Be_{13}$. The creep rates of UBe_{13} show a well-defined linear-in-T dependence from $T=5$ mK up to $T \approx T_c$.[11] They follow the classical temperature dependence predicted by the Kim-Anderson theory.[23] There is no indication for a transition such as the one we observe in the thoriated sample. We conclude that zero creep found in the low-temperature phase is not material dependent, but rather intrinsic to the nature of the low-temperature phase of $U_{0.9725}Th_{0.0275}Be_{13}$.

A similar zero-creep regime was found for the first time by Amann *et al.*[11] in the low-temperature phase of UPt_3. As can be seen from Fig. 9, the strong reduction of creep rates in

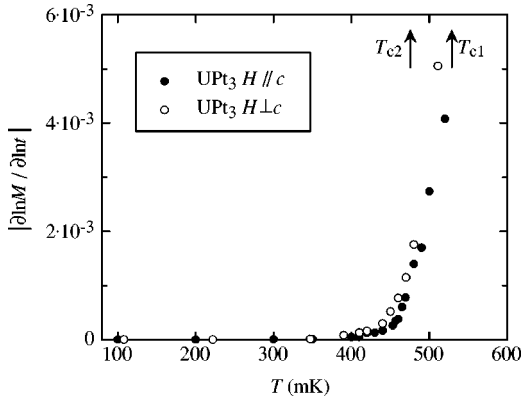

FIG. 9. Normalized initial creep rates of UPt_3, after Ref. 11. The superconducting transition temperatures T_{c1} and T_{c2} of UPt_3 are marked.

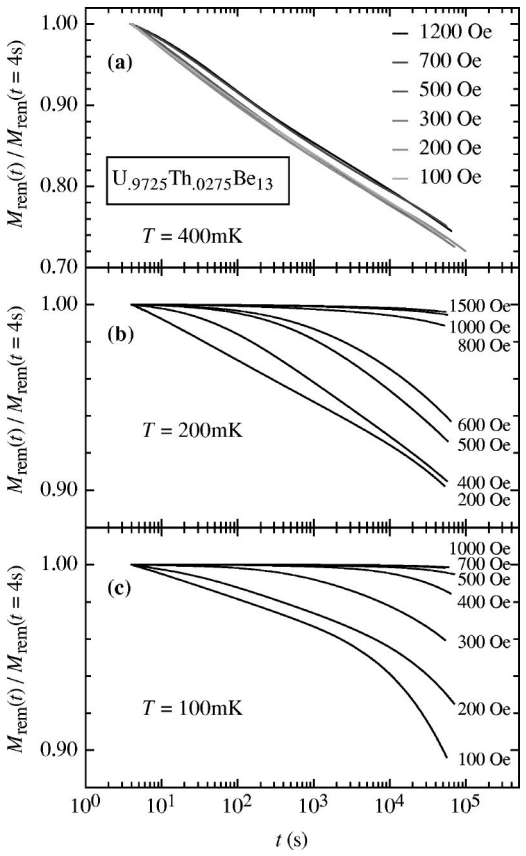

FIG. 10. Relaxation of the remnant magnetization of the $U_{0.9725}Th_{0.0275}Be_{13}$ single crystal for six different cycling fields H_{max} (a) high-temperature phase ($T=400$ mK), (b) low-temperature phase $T=200$ mK, and (c) low-temperature phase $T=100$ mK.

this system also developes just below the second transition to the superconducting phase with broken time-reversal symmetry.

At first sight, the temperature dependence in the high-temperature phase of both systems differs, as can be seen from Figs. 8 and 9. Indeed, in the high-temperature phase of $U_{0.9725}Th_{0.0275}Be_{13}$, the creep rates increase almost linearly with increasing temperature, indicating thermally activated creep. On the other hand, the creep rates of UPt_3 in the high-temperature superconducting phase show a stronger temperature dependence. However, comparing the two figures, one could argue, that this difference is due to the small extent of the high-temperature phase of UPt_3 ($\Delta T_c \approx 50$ mK).

3. Relaxation measurements as a function of cycling field

In this section, we will discuss the influence of the maximum cycling field H_{max} on vortex creep in $U_{0.9725}Th_{0.0275}Be_{13}$. Figure 10 shows decays of $U_{0.9725}Th_{0.0275}Be_{13}$ taken at temperatures both above, and below T_{c2} for different cycling fields.

$T > T_{c2}$. In the high-temperature phase (at $T=400$ mK), the field dependence of the decays is characterized by the following. (i) The decays are logarithmic in time for fields

$100 \leqslant H \leqslant 1200$ Oe. (ii) The fraction of remnant magnetization that decays is the same for all fields.

As can be seen from Fig. 3, this sample enters the fully critical state at $2H^* \approx 500$ Oe. There is no significant difference between decays that started from the undercritical state, or from the fully critical state.

$T < T_{c2}$. A different situation is encountered in the low-temperature phase, where the following features are observed.

At $T = 200$ mK, zero creep is observed only if the sample has been cycled to high-enough fields ($H > 1000$ Oe). As the temperature is reduced, the zero-creep regime is already established at smaller cycling fields. At $T \ll 100$ mK, we observe zero creep for all cycling fields.

From these observations we infer that the pinning strength increases, the more the temperature is reduced below T_{c2}, and the higher the maximum field in which the sample has been cycled before the start of the decay. This is true for the range of field strength applied in this investigation.

4. Field-cooled vs zero-field-cooled relaxation measurements

We have performed field-cooled relaxation measurements on $U_{0.9725}Th_{0.0275}Be_{13}$ at two different temperatures, as a function of cycling fields. In the field-cooled mode, a field H_{max} is applied to the sample at a temperature above T_c. Subsequently, the sample is cooled down to the desired measuring temperature, keeping the field H_{max} constant. When the sample attained thermal equilibrium, the field is reduced to zero in the same way than for zero-field-cooled experiments. The remnant magnetization as a function of time in *zero* field is recorded. After a decay of typically 10^4 s, the sample is warmed up above its transition temperature and the expelled flux is recorded. The remnant magnetization M_{rem} at the start of the decay is given as sum of the decayed plus the expelled flux. Figure 11 shows data above ($T = 400$ mK) and below ($T = 200$ mK) the second transition temperature T_{c2}.

$T > T_{c2}$. In the high-temperature phase, apart from a change in absolute values, there is no qualitative difference between the results obtained in zero-field-cooled and field-cooled mode.

$T < T_{c2}$. In the low-temperature phase, vortex dynamics is considerably altered in field-cooled mode as respect to zero-field cooled:

(i) At $T = 200$ mK zero creep is observed, for $H > 1000$ Oe in zero-field-cooled mode.

(ii) At $T = 200$ mK zero creep is *not* observed, if the sample is field cooled in fields up to 1000 Oe. On the contrary, the decay is strong at high fields and at low fields.

(iii) The field dependence of M_{rem} is different in zero-field and in field-cooled experiments. In zero-field-cooled mode, M_{rem} does not saturate at high fields as would be expected from the Bean model (see also Fig. 3). Instead it goes through a maximum and decreases with increasing fields. In field-cooled mode, the remnant magnetization increases continuously and seems to saturate at high fields. The ''memory effect'' observed in zero-field-cooled mode is not present when the sample has been field cooled, but it rather resembles the behavior for $T > T_{c2}$.

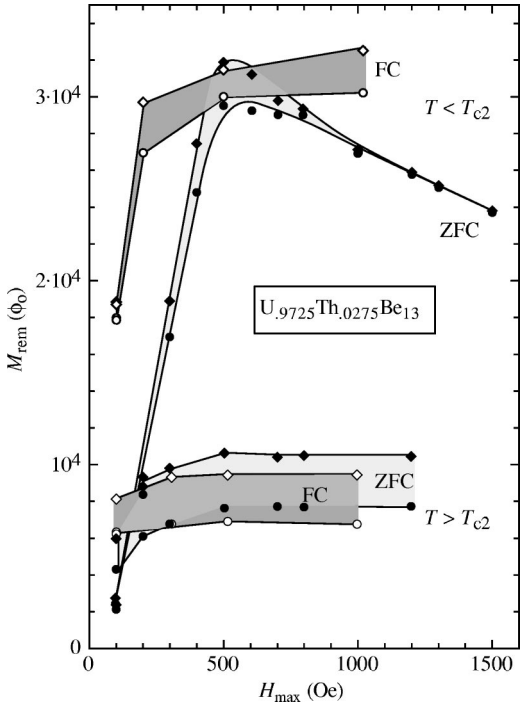

FIG. 11. Comparison between field-cooled (FC) and zero-field-cooled (ZFC) mode, for $T > T_{c2}$ ($T = 400$ mK), and for $T < T_{c2}$ ($T = 200$ mK). Remnant magnetization of the $U_{0.9725}Th_{0.0275}Be_{13}$ single crystal taken at two different times as a function of field. Diamonds are for M_{rem} at the start of the decay measurement ($t \approx 1$ s), and circles for M_{rem} at $t = 10^4$ s. The shaded area indicates the amount of flux that leaves the sample in this time window. The field-cooled data is represented by open symbols and dark shaded area; the zero-field-cooled data by closed symbols and light shaded area.

From these observations we infer that the new pinning mechanism found in the low-temperature phase of $U_{0.9725}Th_{0.0275}Be_{13}$ is not active when field cooling the sample.

B. Flux dynamics in Sr_2RuO_4

1. Remnant magnetization as a function of temperature and field

The field dependence of $M_{rem}(H_{max})$ in Sr_2RuO_4 follows the classical behavior described by the Bean model.[25] At all temperatures, no unusual behavior, such as one observed in thoriated UBe_{13}, is seen in Sr_2RuO_4.

In Fig. 12, the temperature dependence of the remnant magnetization is shown. All the points are taken for cycling fields high enough, so that the sample is in the critical state. According to the Bean model,[25] Fig. 12 represents the temperature dependence of the critical current. It shows, that the critical current varies continuously and saturates for the lowest temperatures. The Bean model allows to give an estimate of the critical current.[25] For the low-T_c sample, we obtain values for the critical current of the order of 10^4 A/cm^2. For

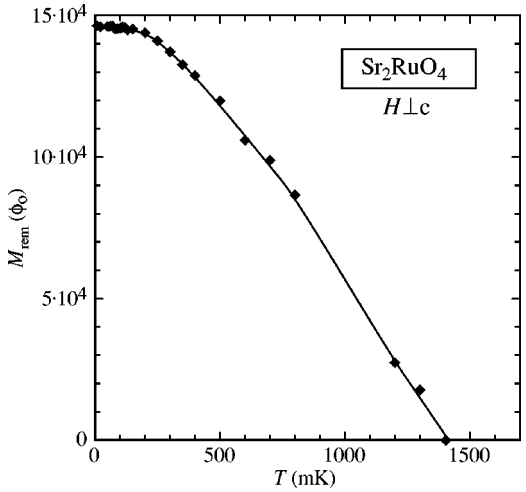

FIG. 12. Remnant magnetization of Sr_2RuO_4 as a function of temperature for sample B ($T_c = 1.4$ K). The line serves as guide to the eyes.

sample B with higher T_c, lower values of the order of 10^3 A/cm^2 have been obtained, which indicates that there are indeed less material defects in this sample.

2. Relaxation measurements as a function of temperature

In this section flux-creep measurements on the low-T_c sample A ($T_c = 1.03$ K), with the field applied both parallel and perpendicular to the c axis, and on the sample B ($T_c = 1.4$ K), with the field applied perpendicular to the c axis, will be presented.

In order to be able to compare relaxation measurements at different temperatures, great care has been taken to ensure, that the starting conditions were identical for all the decays. The samples have been cycled in high-enough fields as to be in the fully critical state. Only in this case, do the flux-density gradients point solely out of the sample. If the sample is not in the fully critical regime, part of the trapped vortices is exposed to a flux-density gradient, and hence to a Lorentz force, pointing towards the inside instead of the outside of the sample. Those vortices relaxing to the inside would probably not leave the sample in our measuring time.

$H \perp c$. In Fig. 13, are plotted typical relaxation measurements for the field applied at an angle of 15° from the ab planes. The following features are observed.

(i) The decays are weak at all temperatures.

(ii) In the first 10^4 s, the decays follow a logarithmic time dependence. After the first 10^4 s, the decays accelerate and follow an unusual nonlogarithmic time dependence.

(iii) Below 26 mK, the vortex creep of the first 10^4 s is practically zero, vortices remain so strongly pinned that they do not escape from the sample in this time range. After the first few hours, some vortices manage to leave the sample.

Let us compare these results to the ones obtained on sample B ($T_c = 1.4$ K) that is about ten times larger than sample A, for H in the ab planes. From Fig. 14 the following observations can be made.

(i) Vortex creep is much *weaker* in sample B ($T_c = 1.4$ K) than in the low-T_c sample A ($T_c = 1.03$ K).

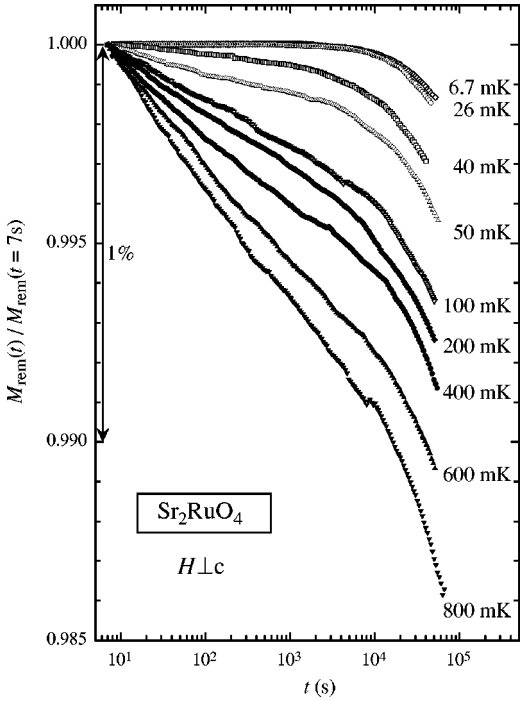

FIG. 13. Relaxation of the remnant magnetization at different temperatures measured on Sr_2RuO_4 ($T_c = 1.03$ K) with the field applied at an angle of 15° from the ab plane.

(ii) For temperatures above 150 mK, the time dependence is practically logarithmic. No such accelerations as observed in sample A are seen in sample B in our time window.

(iii) Below 150 mK, the decays start flattening at short

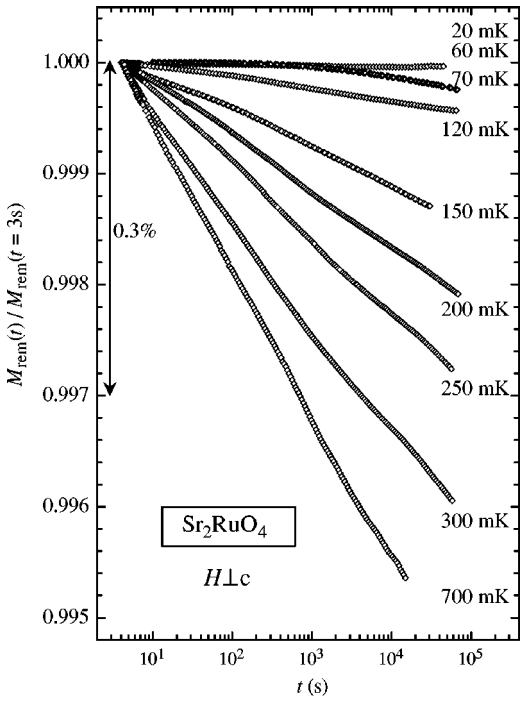

FIG. 14. Relaxation of the remnant magnetization at different temperatures measured on Sr_2RuO_4 ($T_c = 1.4$ K) with the field in the ab plane.

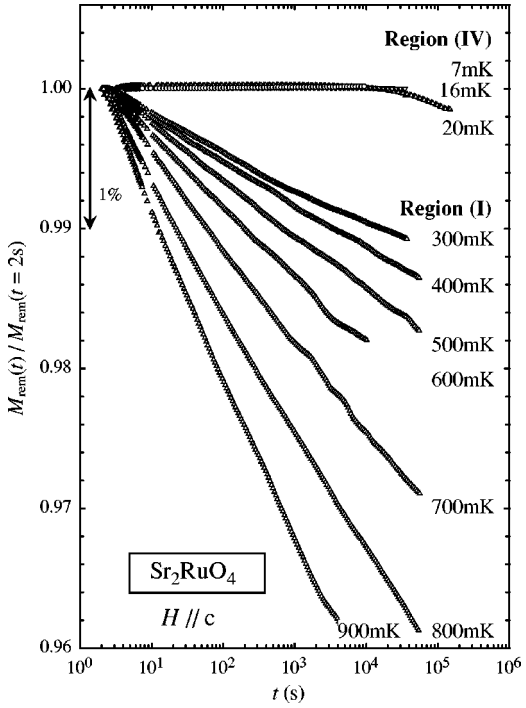

FIG. 15. Relaxation of the remnant magnetization at different temperatures measured on Sr_2RuO_4 ($T_c = 1.03$ K) with the field along the *c* axis: Region (I) 300 mK$<T<$900 mK and region (IV) $T<20$ mK.

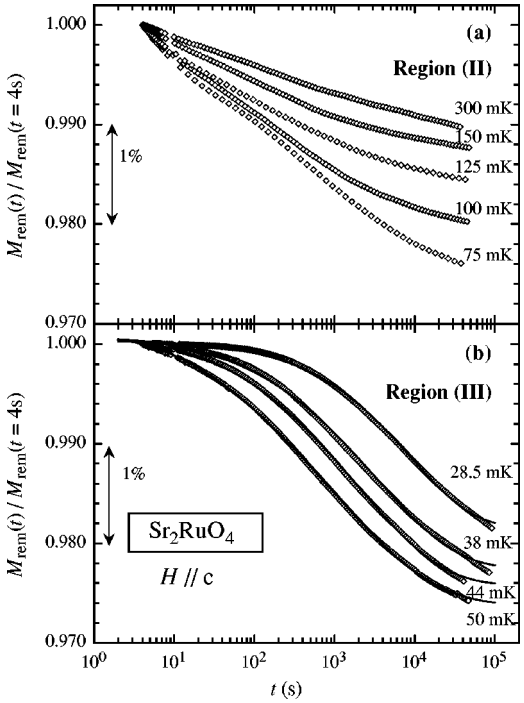

FIG. 16. Relaxation of the remnant magnetization at different temperatures measured on Sr_2RuO_4 ($T_c = 1.03$ K) with the field along the *c* axis. (a) Region II 75 mK$<T<$300 mK. (b) Region III 28.5 mK$<T<$50 mK. Lines are stretched exponential fits.

times and deviate from logarithmic time dependence at longer times [see also Fig. 19(b)].

$H \| c$. The relaxation curves for the configuration with the field parallel to the *c* axis, on the other hand, show very different behavior than the one observed with $H \perp c$. Figures 15 and 16 show decays of sample *A* as a function of temperature with the field oriented along the *c* axis. Four different temperature regimes can be distinguished.

Region (I) in Fig. 15. For temperatures 300 mK$<T<$900 mK, the decays follow a logarithmic time dependence. The fraction of remnant magnetization that decays in our measuring time decreases with decreasing temperature.

Region (II) in Fig. 16(a). In the range 75 mK$<T<$300 mK, the beginning of the decays is logarithmic, but after the first thousands of seconds the relaxation slows down and deviate from the purely logarithmic time dependence. What is remarkable here, is the fact that the fraction of remnant magnetization that leaves the sample in our measuring time *increases* with decreasing temperature.

Region (III) in Fig. 16(b). At low temperatures 28.5 mK$<T<$50 mK, the decays could be fitted to stretched exponentials,

$$M(t) - M(\infty) = [M(0) - M(\infty)] \exp[-(t/\tau)^{\beta}] \qquad (1)$$

with $10^3 < \tau < 10^4$ s and $0.3 < \beta < 0.6$.

It should, however, be noted, that at long times ($t > 30\,000$ s), the decays deviate from the stretched exponential law.

Region (IV) in Fig. 15. At even lower temperatures, for $T<20$ mK, no visible decay could be detected in the first ten thousand of seconds. The vortices remain strongly pinned inside the sample. After this time (approximately 8 h), some vortices manage to escape and leave the sample.

The four different creep regimes are naturally reflected in the initital creep rates plotted in Fig. 17 as a function of temperature, both in linear and semilogarithmic scale.

In the transition regime ($50<T<300$ mK), the decays deviate strongly from the purely logarithmic time dependence. Therefore, the slope $|\partial M / \partial \ln t|$ depends on the chosen fitting range. However, in order to be able to compare the data in this transition regime to the logarithmic decays in the high-temperature regime, we decided to use the slope at short times and extract the initial creep rate

$$\left| \frac{\partial \ln M}{\partial \ln t} \right| \quad \text{for } 10 < t < 100 \text{ s}.$$

Note that this choice affects only the results in the transition regime.

In region (I), the creep rates are decreasing with decreasing temperature. A broad minimum is observed around 300 mK, before the creep rates start increasing again in region (II). Indeed, in this temperature region, the fraction of the remnant magnetization that decays in 10^4 s is increasing with decreasing temperature. Around 60 mK the creep rates reach a local maximum. In the very narrow region (III) vortex creep occurs following approximately stretched exponentials with decreasing strength as the temperature is reduced.

Finally, below 20 mK, the sample enters the zero-creep

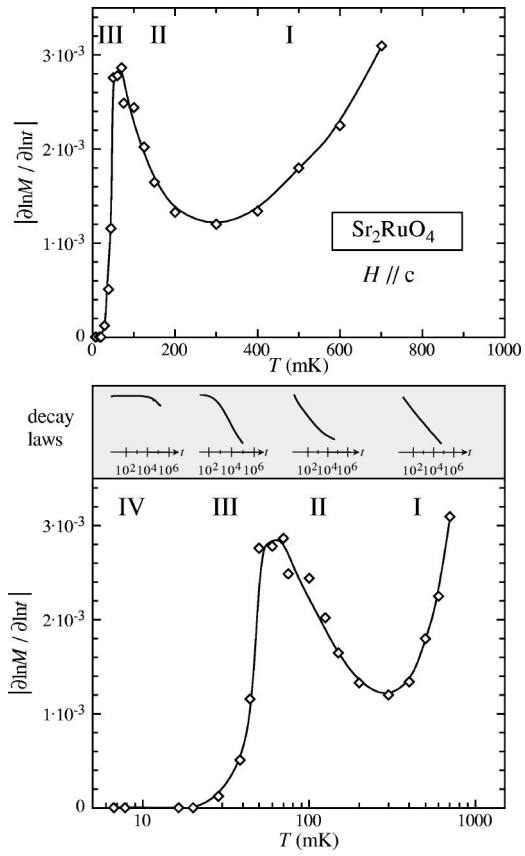

FIG. 17. Normalized initial creep rates of Sr_2RuO_4 ($T_c = 1.03$ K) as a function of temperature. Same data is given in linear and semilogarithmic plot. Regions I–IV correspond to the different creep behaviors described in the text and in Figs. 15 and 16. The lines are guides to the eyes.

regime. The creep rates have dropped by three orders of magnitude to zero within our sensitivity ($|\partial \ln M/\partial \ln t| \approx 2 \times 10^{-6}$).

The temperature dependence of all the measured creep rates for both samples is compared in Fig. 18 in a semilogarithmic plot. In both samples and for both field orientations, the following observations can be made.

(i) Two regimes can be clearly distinguished. A high-temperature regime with creep rates of the order of 0.1%; and a low-temperature regime with zero creep, separated by a strong reduction of creep rates by more than two orders of magnitude, to undetectabely low levels within our sensitivity.

(ii) For the low-T_c sample A ($T_c = 1.03$ K), the two regimes are separated by a rather sharp drop of creep rates around 50 mK for both field directions. However, in sample B ($T_c = 1.4$ K), the drop of creep rates is broadened and shifted to much higher temperatures, around 150 mK. Therefore, the drop in creep rates may be considered to represent a crossover, rather than a transition. The strong pinning mechanism in the high-quality sample does not set in abruptly but increases gradually with decreasing temperature.

(iii) At all temperatures, the creep rates in sample B with higher T_c are much smaller than those of the low-T_c sample, indicating stronger pinning. At first sight one would expect the opposite to be true. If the vortex creep in the high-temperature regime was dominated by extrinsic pinning at crystalline defects, one would expect that the low-T_c sample would show stronger pinning (i.e., lower creep rates). Since the opposite is observed, we conclude that some intrinsic pinning of the same sort than observed at the low-temperature regime might be effective already at higher temperatures.

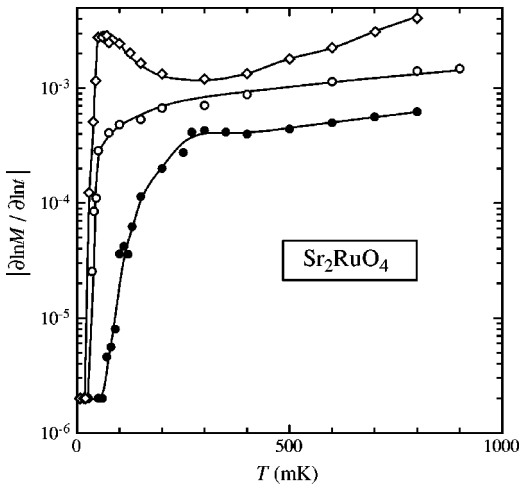

FIG. 18. Normalized initital creep rates of Sr_2RuO_4 as a function of temperature in a semilogarithmic plot. The open symbols represent data of the low-T_c sample A with $T_c = 1.03$ K, and the closed symbols those of sample B with a higher transition temperature of $T_c = 1.4$ K. Circles are for the field perpendicular to the c axis and diamonds for the field parallel to the c axis. The lines are guides to the eyes.

(iv) In the regime of finite creep, the temperature dependence of the rates is different in the two field directions. For fields in the ab plane, the creep rates increase continuously with increasing temperature. In contrast, as we have already discussed, the creep rates for fields along the c axis show a pronounced minimum at $T \approx 300$ mK.

3. Relaxation measurements as a function of cycling field

In Fig. 19 at $T = 700$ mK, we observe no significant difference between decays that started from the undercritical state, and those that start from the fully critical state (see inset of Fig. 19). The time dependence is practically logarithmic for all fields. Moreover, the fraction of vortices that leave the sample in our time interval is the same for all fields.

A completely different situation is encountered in the low-temperature regime, at $T = 70$ mK. As can be seen from Fig. 19(b), the shape and the strength of the decays are strongly field dependent. The lower the maximum cycling field, the larger is the fraction of remnant magnetization that leaves the sample in our measuring time. At this temperature, the fully critical state is realized at $2H^* \approx 200$ Oe. In the undercritical regime, for fields $H < H^*$, the decays follow the classical logarithmic time dependence. For fields $H > 2H^*$, they become more rounded and the initial creep starts flattening. At $H = 600$ Oe, the first 100 s of the decay are practically flat. After the first hundred seconds, some vortices manage to escape from the sample.

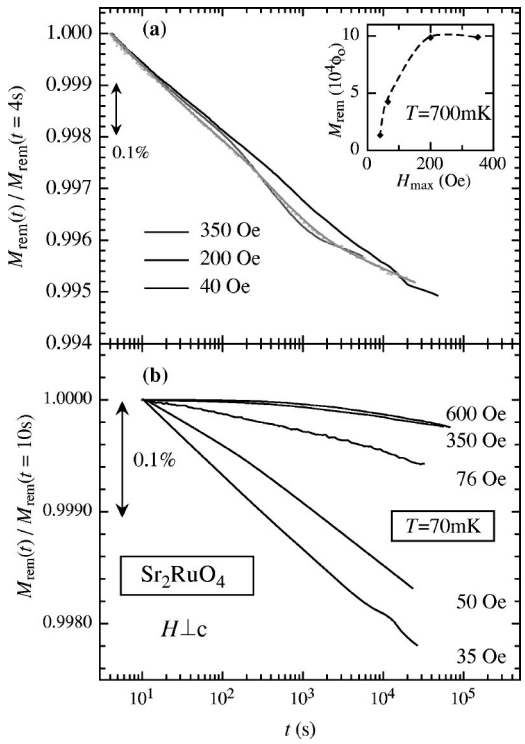

FIG. 19. (a) Relaxation of the remnant magnetization of Sr_2RuO_4 ($T_c = 1.4$ K), as a function of the maximum cycling field H_{max}, at $T = 700$ mK. The inset shows the cycling field dependence of the remnant magnetization. The field is applied pependicular to the c axis. (b) Relaxation of the remnant magnetization as a function of the maximum cycling field H_{max}, at $T = 70$ mK for Sr_2RuO_4 ($T_c = 1.4$ K). At $H_{max} = 200$ Oe the sample is in the fully critical state.

IV. DISCUSSION

In this paper, we address vortex creep in Sr_2RuO_4, thoriated UBe_{13} and compare it to previous work on UPt_3.[11] In all three materials a similar low-temperature vortex creep regime with unusual strong pinning was observed. The latter is so strong, that vortex creep is reduced to zero in a time scale of several hours, therefore, we call this phenomenon zero creep. This is a different type of vortex pinning, very distinct from the conventional pinning due to defects. It is not a property of the material, but it is intrinsic to the superconducting phase in question.

Although vortex dynamics shows many characteristics specific to each superconductor, a zero-creep regime is observed in all the three materials with the following common features.

(i) Vortices remain so strongly pinned that no creep is observed in the first few hours.

(ii) Several hours after the start of the decay, some vortices manage to escape and leave the sample. As the temperature is reduced these accelerations occur at longer and longer waiting times.

(iii) The pinning strength increases gradually with decreasing temperature and increasing cycling field.

(iv) Although vortex creep goes to zero, no dramatic increase of the critical current is observed.

An interpretation of these phenomena, not observed in any other type-II superconductor, has been proposed by Sigrist and Agterberg.[9] In their model, they consider a time-reversal symmetry-breaking phase with two different degenerate superconducting states separated by a domain wall. A vortex approaching such a domain wall, decays into fractional vortices, each carrying only a fraction of Φ_o with the sum of their fluxes being equal to Φ_o. Because the sum of their line energies is lower than that of a conventional vortex with one flux quantum, they do not recombine and leave the domain walls. Since vortices repel each other, these domain walls occupied with fractional vortices, can act like ''fences'' for oncoming conventional vortices.[9] This pinning phenomenon would explain our observation of zero creep.

The described mechanism is *intrinsic*, originating from the nature of the superconducting state itself. Pinning by domain walls should not influence the magnitude of the critical current. The latter is governed by extrinsic pinning, due to defects of the crystal. This is in accordance with our observations.

Further support for the formation of domain walls is given by ac-susceptibilty measurements performed by Amann *et al.*[11] on a UPt_3 single crystal. They revealed a second peak at T_{c2} in the out-of-phase component χ''. The peak does not depend on the frequency of the measuring field but rather on its amplitude: With increasing amplitude, the maximum of the peak is shifted towards lower temperatures and its width increases. It was concluded, that it might be related to the motion of domain walls and/or fractional vortices building up in the B phase of UPt_3.[11]

In the picture of Sigrist and Agterberg,[9] a domain wall close to the surface may open some escape channels for the vortices due to their pressure. With time this channels expand more and more, so the process accelerates. This process is strongly temperature dependent (domain wall dynamics). The starting time of the acceleration increases as the temperature is reduced below T_{c2}. Motion of domain walls is also supported by recent hysteresis measurements in a slowly oscillating magnetic field by the Rosenbaum group[26] on a UPt_3 single crystal.

Domains are believed to nucleate randomly at the superconducting transition temperature that leads to a time-reversal-symmetry-violating state, *unless* there is bias for one type of domain. In time-reversal-symmetry-breaking superconducting phases, an external magnetic field could provide such a bias. Therefore, field-cooling the sample would result in a smaller number but in bigger domains than in the zero-field-cooled process. This is due to the fact that the magnetic field may ''polarize'' the superconducting order parameter, thus leading to a preferred domain type. The pinning should then be stronger in the zero-field-cooled case due to a larger number of domain walls.

This has been observed in our field-cooled relaxation experiments on $U_{0.9725}Th_{0.0275}Be_{13}$. Whereas in the high-temperature phase, there is no qualitative difference between the results obtained in zero-field-cooled and field-cooled mode, the intrinsic pinning mechanism found in the low-temperature phase in the zero-field-cooled mode, is not activated in field-cooled relaxation experiments. Indeed, we do

not observe zero creep in the time-reversal-symmetry-breaking phase if the sample has been field cooled. On the contrary vortex creep remains strong even at high fields. A similar conclusion has been made from a different type of investigation by the Rosenbaum group in thoriated UBe_{13}.[27]

In the following we discuss the dependence of the decays on the cycling field strength.

(i) In $U_{0.9725}Th_{0.0275}Be_{13}$ and Sr_2RuO_4, we observe that for low cycling fields, which introduce vortices close to the surface, we do not have zero creep. The observed relaxation in that case is due to vortices at the surface, which are not impeded by the barriers and leave the sample when the magnetic field is turned off. This was already observed by Amann *et al.*[11] in UPt_3. It was argued that the observed strong decays at low cycling fields—following stretched exponential law—resulted from the motion of vortices at the surface. This argument was supported by measurements on UPt_3 powder. In the powder sample, strong stretched exponential decays were observed for every field strength. In fact, no zero-creep regime was observed in the powder sample. Probably the powder grains are too small for domain walls to form and/or efficiently inhibit vortex motion.

(ii) In the low-temperature phase of UPt_3, the zero-creep regime is already established at very low fields (undercritical state) even for temperatures close to the second transition temperature T_{c2}. On the other hand in $U_{0.9725}Th_{0.0275}Be_{13}$ and Sr_2RuO_4, rather high cycling fields have to be applied to the sample, before we observe zero creep. For temperatures just below the transition to the zero-creep regime, fields higher than the critical field of the Bean model are necessary to activate the novel pinning mechanism. As the temperature is further reduced, smaller cycling fields are needed to establish the zero-creep regime.

Our observation of zero-creep can be interpreted as an indirect evidence for the existence of domain walls and fractional vortices in the low-temperature phase of UPt_3 and $U_{0.9725}Th_{0.0275}Be_{13}$ and in Sr_2RuO_4 at the lowest temperatures. So far, a direct observation of domain walls occupied by fractional vortices has not been made. In the last ten years, scanning tunneling or magnetic force microscopy have been successfully applied to image (standard) vortices in $NbSe_2$[28] and $YBa_2Cu_3O_{7-\delta}$.[29] Unfortunately, the relatively low temperatures needed to apply this sort of techniques to UPt_3, thoriated UBe_{13}, and Sr_2RuO_4 (the interesting temperature range lies below 0.5 K), and problems with surface preparation, could delay the search for domain walls and/or fractional vortices.

V. SUMMARY AND CONCLUSION

Summarizing, we have found a pinning mechanism in the low-temperature phase of $U_{0.9725}Th_{0.0275}Be_{13}$ similar to the one observed in UPt_3,[11] and in Sr_2RuO_4 at the lowest temperature. It is very distinct from the standard pinning by defects. It results in a completely different vortex dynamics than the one observed in classical, or in high-T_c superconductors. The pinning mechanism is so strong that no vortex creep is observed in a time scale of several hours. After this time period, some vortices close to the surface escape. We observe that the pinning strength increases with increasing cycling field and with decreasing temperature. This pinning mechanism is not material dependent, but rather intrinsic to unconventional superconducting states. Our observations can be explained in the framework of the theoretical model by Sigrist and Agterberg.[9]

In the case of UPt_3 and $U_{0.9725}Th_{0.0275}Be_{13}$, the pinning regime coincides with their respective low-temperature phases that violate time-reversal symmetry.[4,5,3] In contrast, the reduction of vortex creep in Sr_2RuO_4 does not set in right below the superconducting transition temperature where the breakdown of time-reversal symmetry has been observed,[6] but it occurs only at much lower temperatures. In this material, the drop in creep rates might be associated with a ''transition'' of domain wall states attributable to the multiband nature of the superconducting state in Sr_2RuO_4.[9]

ACKNOWLEDGMENTS

We acknowledge many fruitful discussions with Maurice Rice, Manfred Sigrist, and Daniel Agterberg. We thank Andreas Amann for his invaluable help during the first series of measurements on Sr_2RuO_4 and thoriated UBe_{13} and for many enlightening discussions. We also acknowledge Andreas Baumgartner, Maurizio Leonardi, and Marc von Waldkirch for their help in acquiring the data. This work would have been impossible without high quality samples; we are, therefore, deeply grateful to Y. Maeno for providing Sr_2RuO_4 single crystals and to J.L. Smith for the thoriated UBe_{13} single crystal. We acknowledge partial financial support from the ''Schweizerischer Nationalfonds zur Foerderung der Wissenschaftlichen Forschung.''

[1] A.J. Legget, Nature (London) **270**, 585 (1977).
[2] D.N. Paulson and J.C. Wheatley, Phys. Rev. Lett. **40**, 557 (1978).
[3] G.M. Luke, A. Keren, L.P. Le, W.D. Wu, Y.J. Uemura, D.A. Bonn, L. Taillefer, and J.D. Garrett, Phys. Rev. Lett. **71**, 1466 (1993).
[4] R.H. Heffner, J.O. Willis, J.L. Smith, P. Birrer, C. Baines, F.N. Gygax, B. Hitti, E. Lippelt, H.R. Ott, A. Schenck, and D.E. Laughlin, Phys. Rev. B **40**, 806 (1989).
[5] R.H. Heffner, J.L. Smith, J.O. Willis, P. Birrer, C. Baines, F.N. Gygax, B. Hitti, E. Lippelt, H.R. Ott, A. Schenck, E.A. Knetsch, J.A. Mydosh, and D.E. MacLaughlin, Phys. Rev. Lett. **65**, 2816 (1990).
[6] G.M. Luke, Y. Fudamoto, K.M. Kojima, M.I. Larkin, J. Merrin, B. Nachumi, Y.J. Uemura, Y. Maeno, Z.Q. Mao, Y. Mori, H. Nakamura, and M. Sigrist, Nature (London) **394**, 558 (1998).
[7] O.V. Lounasmaa and E. Thuneberg, Proc. Natl. Acad. Sci. U.S.A. **96**, 7760 (1999), and references cited therein.
[8] M. Sigrist and K. Ueda, Rev. Mod. Phys. **63**, 239 (1991).
[9] M. Sigrist and D.F. Agterberg, Prog. Theor. Phys. **102**, 965 (1999).

[10] M. Sigrist and T.M. Rice, Phys. Rev. B **39**, 2200 (1989).
[11] A. Amann, A.C. Mota, M.B. Maple, and H. von Löhneysen, Phys. Rev. B **57**, 3640 (1998).
[12] A.C. Mota, E. Dumont, and J.L. Smith, J. Low Temp. Phys. **177**, 1477 (1999).
[13] E. Dumont, A.C. Mota, and J.L. Smith, Physica B **284–288**, 525 (2000).
[14] A.C. Mota, E. Dumont, J.L. Smith, and Y. Maeno, Physica C **332**, 272 (2000).
[15] Y. Maeno, H. Hashimoto, K. Yoshida, S. Nishizaki, T. Fujita, J.G. Bednorz, and F. Lichtenberg, Nature (London) **372**, 532 (1994).
[16] T.M. Rice and M. Sigrist, J. Phys.: Condens. Matter **7**, L643 (1995).
[17] T.M. Rice, Nature (London) **396**, 627 (1999).
[18] A.C. Mota, E. Dumont, A. Amann, and Y. Maeno, Physica B **259-261**, 934 (1999).
[19] A.C. Mota, P. Visani, and A. Pollini, J. Low Temp. Phys. **76**, 465 (1989).
[20] J.L. Smith, Philos. Mag. B **65**, 1367 (1992).
[21] A. Ramirez (private communication).
[22] Y. Kim, C.F. Hempstead, and A.R. Strand, Phys. Rev. Lett. **9**, 306 (1962).
[23] P.W. Anderson, Phys. Rev. Lett. **9**, 309 (1962).
[24] U. Rauchschwalbe, F. Steglich, G.R. Stewart, A.L. Giorgi, P. Fulde, and K. Maki, Europhys. Lett. **3**, 751 (1987).
[25] C.P. Bean, Phys. Rev. Lett. **8**, 250 (1962).
[26] E. Shung, T.F. Rosenbaum, and M. Sigrist, Phys. Rev. Lett. **80**, 1078 (1999).
[27] R.J. Zieve, T.F. Rosenbaum, J.S. Kim, G.R. Stewart, and M. Sigrist, Phys. Rev. B **51**, 12 041 (1995).
[28] H.F. Hess, R.B. Robinson, R.C. Dynes, J.M. Valles, and J.V. Waszczak, Phys. Rev. Lett. **62**, 214 (1989).
[29] A. Mosera, H.J. Hug, I. Parashikov, B. Stiefel, O. Fritz, H. Thomas, A. Baratoff, H.J. Güntherodt, and P. Chaudhari, Phys. Rev. Lett. **74**, 1847 (1995).